Influence of rare earth treatment on interfacial properties of carbon fiber/epoxy composites

Zhiwei Xu, Yudong Huang *, Chunhua Zhang, Gang Chen

Department of Applied Chemistry, Harbin Institute of Technology, P.O. Box 410, Harbin Heilongjiang 150001, China

Abstract

In this work, the effect of soaking and irradiating in praseodymium nitrate solution on the surface physicochemical properties of carbon fibers and interfacial properties of composites has been investigated, and the interfacial adhesion mechanism of treated carbon fiber/epoxy composite was analyzed. It was found that both of immersion and irradiation lead to an increase of fiber surface roughness, improvement of oxygen-containing groups, enhancement of disorder degree and introduction of praseodymium element on carbon fiber surface. As a result, the coordination linkage between fibers, praseodymium ion and matrix is formed and the interlaminar shear strength (ILSS) of composites is increased, due to the improvement of interfacial adhesion between fibers and matrix resin. Moreover, γ-ray irradiation treatment is superior to immersion treatment in promoting interfacial properties owing to the increase of carboxyl and carbonyl.
© 2006 Elsevier B.V. All rights reserved.

Keywords: Rare earth; Carbon fiber/epoxy composite; Interfacial properties; X-ray photoelectron spectroscopy

1. Introduction

Polymer matrix composites are the main application of carbon fibers. The interface between carbon fibers and resin matrix plays a critical role in controlling the overall properties of the composites, such as off-axis strength, fracture toughness and environment stabilities. Interfacial characteristics determine the way loads can be transferred from the polymer to the fiber, and are often quantified in terms of the so-called interlaminar shear strength (ILSS). Below a certain critical strength, the surface of the fibers is not sufficient for the transfer to occur adequately. However, the inertness characteristics of carbon fiber surface usually result in inferior wettability and weak adhesion between the fibers and resin [1–3]. As a result, it is necessary to treat or modify the surface of carbon fibers in their application.

A literature survey shows that a range of experimental techniques have been applied to modify the surface of carbon fibers, including anodization, plasma treatment and solution and gas phase oxidation [1,4–7]. Most modifications on the interfacial properties of carbon composites have been focused on increasing the surface free energy or introducing organic groups on the

fibers, and the interfacial property was improved at all levels after modification.

Rare earth compounds have been widely used in optics, electronics, metallurgy and chemical engineering because of their special characteristics [8–12]. During the past several decades, most investigations were focused on the effect and application of rare earth elements for the metal surfaces, and a few were related to using rare earth elements as non-metal material surface modifier [13–15]. In particular, less information is available about applying the rare earth elements for the surface treatment of carbon fiber, as well as the effect of rare earth elements on the adhesive property of carbon fiber composites.

The purpose of the present work is to evaluate the surface treatment of carbon fibers by means of $Pr(NO_3)_3$ solution, investigate the effect of different surface treatment conditions on interfacial properties of carbon/epoxy composites and relate them with the interfacial behavior in polymer matrix composites.

2. Experimental

2.1. Preparation

The polyacrylonitrile (PAN) based carbon fibers with kidney-type cross-section investigated in current studies were

* Corresponding author. Tel.: +86 451 86413711; fax: +86 451 86413711.
  E-mail address: xushuangxuan@163.com (Y. Huang).

supplied by Institute of Coal Chemistry, CAS (the average width is $9\,\mu m$ and the thickness is $3\,\mu m$, linear mass is $0.0627\,g^{-1}$). Praseodymium nitrate was prepared by dissolving praseodymium oxide (purchased from Shanghai Chemical Reagent Co.) in nitric acid. The matrix system used was E-618 epoxy resin system consisting of diglycidyl ether of bisphenol-A (supplied from Yue-Yang Chem. Co. of China), curing agent: phthalic anhydride and benzyl dimethylamine at 100, 70 and 1 parts by weight, respectively. The irradiation field was provided by Harbin Rui Pu Irradiation Technology Company of China. The intensity of Co^{60} γ-ray source was 1.5×10^4 Ci and the dose rate was 6.0×10^3 Gy/h.

Two types of surface modification methods were used: soaking the carbon fibers in the 0.5 wt% water solution of praseodymium nitrate and irradiating the mixture of carbon fibers and 0.5 wt% water solution of praseodymium nitrate by γ-ray.

Before treatment, fibers were extracted to remove coating on fiber surface. Then fibers were put in a plastic container and vacuumized. The praseodymium nitrate/water solution was inhaled into the container under negative pressure and the fibers were wholly immersed. The carbon fibers were dipped into the solution of $Pr(NO_3)_3$ for 6 h, and then dried for 2 h at 120 °C. The mixture of carbon fibers and praseodymium nitrate solution was irradiated by γ-ray for the dose of 3×10^5 Gy and the carbon fibers were dried for 2 h at 120 °C.

Using the carbon fibers and epoxy resin, the prepreg was paid unidirectional into a mold to manufacture composites. The prepreg was pressed and cured under 5 MPa pressure for 2 h at 90 °C, under 10 MPa pressure for 2 h at 120 °C and under 10 MPa pressure for 4 h at 150 °C by hot-press machine and we could obtain specimens with fiber mass fraction of 63($\pm$1.5%).

2.2. Measurements

The morphology of fiber surface and failure of fiber-reinforced composites were inspected by scanning electron microscopy (SEM) FEI SIRION 200 before and after treatment. ESCA (Lab220i-XL) made in V.G. Scientific Company, U.K. and equipped with a Al Kα (1.25 keV) radiation source generated at 12 kV and 20 mA, was used to determine composition of fiber surface.

The Raman spectrometer used was a Renishaw 2000 and the monochromatic light source was an Ar$^+$ laser (514.5 nm). The laser beam, polarized parallel to the fibers axis, was focused on the samples with the 50$\times$ objective onto a spot 1–2 μm in diameter. Before X-ray photoelectron spectroscopy (XPS) and Raman spectrometer tests, untreated and treated carbon fibers were both extracted with acetone for 48 h in order to wash out impurities on their surface.

ILSS of composites was measured by short-beam bending test according to ASTM D-2344 using an Instron 1125. A span-to-depth ratio of 5:1, a cross-head speed of 2 mm min^{-1}, and a sample thickness of 2 mm were used. More than eight specimens were tested for each of the composites studied and the average value was taken in the present work studied.
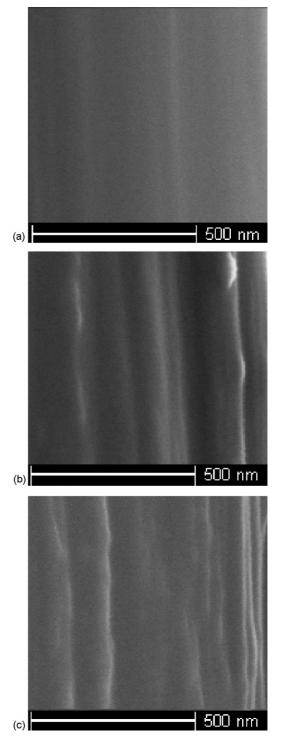

Fig. 1. Microscopic images of carbon fibers before and after treatment: (a) untreated; (b) immersion treated; (c) irradiation treated.

3. Results and discussion

3.1. Surface topography of fibers

The SEM images of the original, immersion treated and irradiation treated carbon fibers are shown in Fig. 1a–c, respectively. Compared to the original carbon fiber, the treated carbon fiber surface is rougher, some granules are formed and the grooves of
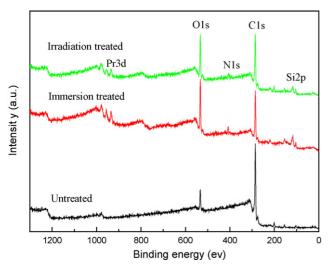
Fig. 2. Wide scan XPS spectra of untreated and treated carbon fibers.

Table 1
Variation of surface composition of the carbon fibers before and after treatment

	C (%)	O (%)	Pr (%)	N (%)	Si (%)
Untreated	85.42	11.61	0	0	2.97
Immersion treated	54.93	34.78	1.77	4.08	4.44
Irradiation treated	60.72	29.49	1.74	3.80	4.25

fiber surface become wider and deeper. Moreover, the immersed carbon fiber shows a more distinct increase in roughening and depth of grooves than the irradiated fiber. It is indicated that the praseodymium ion etches the carbon fiber surface properly and γ-ray irradiation etches the carbon fiber surface excessively.

3.2. Surface composition of fibers

It is well known that XPS is a very useful technique in the determination of chemical composition and functional groups of fiber surface and the maximal XPS sampling depth is ~6 nm. Wide scan spectra in the binding energy range 0–1350 eV were obtained to identify the surface elements present and carry out a quantitative analysis (Fig. 2). The XPS spectra show distinct carbon and oxygen peaks, representing the major constituents of the carbon fibers investigated. Praseodymium and nitrogen elements were detected from the spectroscopy of carbon fibers treated. A small amount of silicon was also observed as the impurity. The surface composition of untreated, immersion treated and irradiation treated carbon fibers was determined by XPS and the results are given in Table 1.

As shown in Table 1, the amount of surface oxygen is increased, the amount of surface carbon is decreased and the elements of praseodymium and nitrogen are detected after treatment. An about three-fold increase in oxygen content occurs after rare earth treatment. The large variation of oxygen groups may be attributed to the oxidation of carbon fibers by praseodymium ion and introduction of nitrate ion. It is deduced that interfacial adhesion between the carbon fibers and matrix is improved when the carbon fiber is treated with rare earth, which results in the promotion of interface properties.

Fig. 3a–c presents C_{1s} and O_{1s} envelopes for the virgin and treated fibers. It can be noticed that the total fraction of the C_{1s} envelope associated with oxygen environments (shoulders located on the high energy side of the main peak at 284.8 eV) is greater for the samples processed by rare earth treatment. However, XPS is not capable of resolving the individual contributions of functionalities such as hydroxyl-ester, carbonyl, carboxyl, anhydrides or lactose. Following previous work in the literature, a semi-quantitative description of the differences was attempted using a curve-fitting deconvolution procedure [16].

The carbon peaks, which were observed in the binding energy range from 280 to 295 ev, can be attributed to several carbon-based surface functional groups that have different binding energies. The C_{1s} peak of each carbon fiber sample was analyzed using a peak synthesis procedure, which combines Gaussian and Lorentzian functions. The intensity contribution of each functional component peak was estimated by a computer simulation [17,18].

The narrow scan spectra of the C_{1s} region deconvoluted into surface functional group contributions are shown in Fig. 3a–c for the untreated, immersion treated and irradiation treated carbon fibers, respectively. The binding energy value and percent contribution of each curve fit photopeak were estimated from these curve fit C_{1s} photopeaks and are listed in Table 2. Deconvolution of the C_{1s} spectra of carbon fibers gave four peaks designated as peak A (at 284.7–284.9 eV assigned to graphitic carbon), peak B (at 285.5–285.8 eV, carbon bonded phenolic or alcoholic hydroxyls or ether oxygens), peak C (at 286.7–286.8 eV, carbonyl carbon in ketones and quinines) and peak D (at 288.7–288.8 eV, carboxyl functions or ester groups) [19–21].

Close examination of the graphite carbon peak A showed that the full width at half maximum (FWHM) were increased from about 1.4 to 1.48 eV following the immersion treatment and 1.52 eV following the irradiation treatment, suggesting that disordering of the carbon lattice might result from treatment. This also indicates that higher microporosity is correlated with decreasing graphitic character of the surface region [22].

Table 2
Relative content of functional groups in C_{1s} spectra from XPS (peak A, C—C; peak B, C—OH/C—O—C; peak C, C=O; peak D, COOR/COOH)

	Peak A		Peak B		Peak C		Peak D	
	P.C. (%)	B.E. (eV)	P.C. (%)	B.E. (eV)	P.C. (%)	B.E. (eV)	P.C. (%)	B.E. (eV)
Untreated	49.7	284.73	31.9	285.77	12.9	286.83	5.5	288.77
Immersion treated	42.3	284.84	22.5	285.57	17.8	286.73	17.4	288.82
Irradiation treated	32.1	284.85	25.8	285.54	23.1	286.82	19.0	288.71

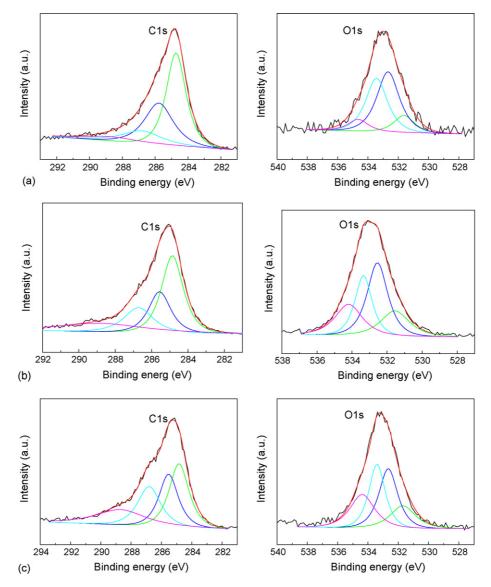P.C.: percentage contribution; B.E.: binding energy.

Fig. 3. C_{1s} and O_{1s} XPS spectra of carbon fibers untreated and treated: (a) untreated; (b) immersion treated; (c) irradiation treated.

From these results, it is clear that the carbonyl carbon in ketones and quinines (C=O) and carboxyl functions or ester groups (COOH/COOR) functional groups increase, and the graphitic carbon (C–C) and carbon bonded phenolic or alcoholic hydroxyls or ether oxygens (C–OH/C–O–C) functional groups decrease after treatment. Furthermore, the oxygen functional group percentage of carbon fibers treated by irradiating is greater than that of carbon fibers treated by soaking. This result may be attributed to the γ-ray irradiation inducing free radical reaction between carbon fiber surface and oxygen dissolved in solution [23].

The interpretation of the O_{1s} spectrum is not so straightforward because the relaxation energies associated with O_{1s} core ionization are not a simple function of structure; in addition, O_{1s} and C_{1s} regions probe different depths into the surface. Nevertheless, we tentatively used peak assignments given by Zielke et al. [24].

Similar deconvolution of the O_{1s} spectra gave four peaks, designated as peak I (at 531.5–531.7 eV, quinoid carbonyl oxy-

gen), peak II (at 532.5–532.7 eV, carbonyl oxygen atoms in esters, amides, anhydrides and oxygen atoms in hydroxyls or ethers, peak III (at 533.3–533.4 eV, the non-carbonyl (ether-type) oxygen atoms in esters and anhydrides) and peak IV (at 534.2–534.7 eV, oxygen atoms in carboxyl groups) [20,21]. From these data, the relative distributions of the functional groups from the O_{1s} spectra were calculated and are shown in Table 3 for each sample.

As Fig. 3a–c shows, a shift of the O_{1s} spectrum toward higher binding energy occurs following the immersion and irradiation treatment. Such a shift can be correlated with the carbonyl band in the C_{1s} core-level spectra [25]. Accordingly, the carboxyl band occurring at 534.2–534.7 becomes surprisingly stronger upon rare earth treatment, as shown in Table 3, reaching after the immersion and irradiation treatments as much as 20.5% and 23.2%, respectively, of the total O_{1s} intensity in comparison with only 6.9% for the parent carbon fiber. This is somewhat in accordance with the above-discussed sequence for the intensity of the 288.7–288.8 eV peak (carboxyl or ester groups) in the

Table 3
Relative content of functional groups in O_{1s} spectra from XPS (peak I, C=O; peak II, carbonyl oxygen atoms in esters, amides, anhydrides and oxygen atoms in hydroxyls or ethers; peak III, non-carbonyl (ether-type) oxygen atoms in esters and anhydrides; peak IV, COOH)

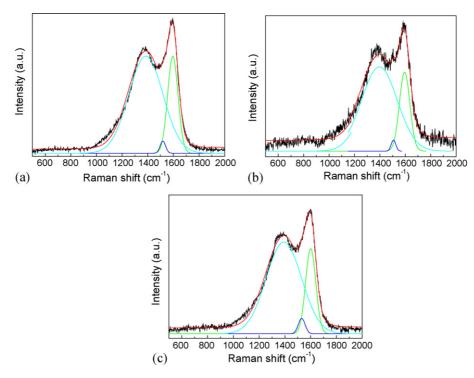|	Peak I		Peak II		Peak III		Peak IV	
	P.C. (%)	B.E. (eV)	P.C. (%)	B.E. (eV)	P.C. (%)	B.E. (eV)	P.C. (%)	B.E. (eV)
Untreated	11.5	531.62	44.6	532.67	37.0	533.40	6.9	534.65
Immersion treated	17.4	531.55	37.0	532.55	25.1	533.34	20.5	534.19
Irradiation treated	17.8	531.69	30.6	532.66	28.4	533.40	23.2	534.38

P.C.: percentage contribution; B.E.: binding energy.

Fig. 4. Deconvolution of Raman spectra of untreated and treated carbon fibers: (a) untreated; (b) immersion treated; (c) irradiation treated.

C_{1s} spectrum. Rare earth treatment, relatively, seems to have caused the increase of quinoid carbonyl functions (peak I of O_{1s} spectra). In addition, rare earth treatment promoted the reduction of peak II in the O_{1s} spectra (carbonyl oxygen atoms in esters, amides, anhydrides and oxygen atoms in hydroxyls or ethers). Also, there is a decrease in the ester/anhydride (peak III).

Raman microprobe spectrometry can be used as a tool for the surface characterization of partially ordered carbon materials, with an estimated analysis depth of 100 nm. Rare earth treatment is expected to introduce some degree of surface disorder measurable by Raman spectrometry. The first-order spectrum presents for all studies samples two relatively broad bands central at ∼1580 and ∼1380 cm^{-1} and a heavy overlapping between them (a situation typical of poorly organized material). Band positions were analyzed using a mixed Gaussian–Lorentzian curve-fitting procedure in Fig. 4. As found previously for a variety of disordered carbon materials [26,27], the best curve fitting was obtained using mixtures of Gaussian and Lorentzian line shape with three bands at 1595–1600 cm^{-1} (G band, typical of graphitic order), 1381–1391 cm^{-1} (D band, typical of structural disorder and defects) and 1508–1530 cm^{-1} (D″ band, associated with amorphous SP^2-bonded forms of carbon or interstitial

defects [20,27]). The second-order Raman envelope was very weak, typical for disordered carbons.

The positions, widths and relative intensities of the different bands constituting the first-order spectra are given in Table 4
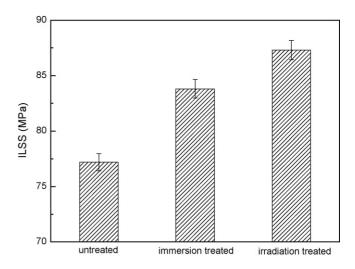

Fig. 5. Effect of treatment methods on ILSS of carbon fiber/epoxy composites.

Table 4
Relative intensities (*I*), position (*V*) and widths (*W*) of the different bands in the first-order Raman spectra of selected samples

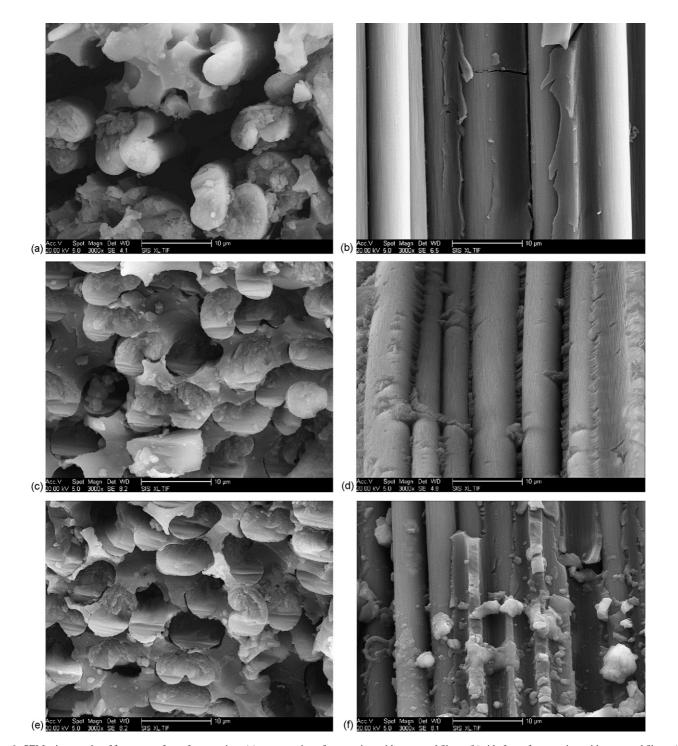|	V_G (cm^{-1})	W_G (cm^{-1})	V_D (cm^{-1})	W_D (cm^{-1})	V_D'' (cm^{-1})	W_D'' (cm^{-1})	W_D/W_G	I_D/I_G
Untreated	1596	95.5	1381	314.7	1518	50.0	3.30	3.31
Immersion treated	1595	96.9	1391	331.6	1508	41.9	3.42	3.66
Irradiation treated	1600	93.1	1387	323.9	1530	62.0	3.48	3.75

Fig. 6. SEM micrographs of fracture surface of composites: (a) cross-section of composites with untreated fibers; (b) side face of composites with untreated fibers; (c) cross-section of composites with immersion treated fibers; (d) side face of composites with immersion treated fibers; (e) cross-section of composites with irradiation treated fibers; (f) side face of composites with irradiation treated fibers.

(all of these parameters have been shown to be suitable indicators for the degree of structural order in carbon materials). The large values found for the D-band width at half maximum (W_D) indicate a highly disordered carbon microstructure. It can also be noticed that various peak parameters change somewhat upon rare earth etching and oxidation. As Table 4 shows, rare earth treatments in general brought about a slight rise in the I_D/I_G and W_D/W_G ratios, indicative of an increase in the degree of disorder [28], which would occur through the breaking of aromatic bonds and the reduction of surface crystallinity [29]. This is more evident in the spectra obtained using irradiation treatment, which may be considered as more reliable than those obtained using immersion treatment.

3.3. Interfacial properties of composites

The ILSS results of composites reinforced by carbon fibers treated in different methods are shown in Fig. 5. After surface treatment, the ILSS values of composites are enhanced by 8.5% (immersion treatment) and 13.1% (irradiation treatment), respectively compared with the untreated carbon fiber composites. The chemical bonding and mechanical interlocking between carbon fibers and matrix resin can be responsible for these results. It is indicated that irradiation treatment by rare earth is more effective than immersion treatment in improving the interfacial adhesion of carbon fiber/epoxy composites.

3.4. Fracture surface topography of composites

Representative topographic features of untreated and rare earth-treated carbon fiber/epoxy composites are shown in Fig. 6.

There is a marked difference in surface topography between untreated and treated fiber composites. From the figures, it can be seen that the fracture surface of the composite with the untreated carbon fiber exhibits a brush-like appearance and poor interfacial bonding. The fibers were pulled out of the resin matrix (Fig. 6a and b). The interfacial bonding of composites with soaking-treated carbon fibers appears to have been obviously improved as can be seen in Fig. 6c and d. Irradiating-treated carbon fiber composites show less fiber pull-out and the matrix is engulfed by fibers, which allows the matrix to secure more bonds and better adhesive force between two phases, which can effectively transfer the load applied to the fiber-reinforced composite system (Fig. 6e and f).

3.5. Mechanism of interfacial adhesion improvement

According to the chemical bonding theory and the interdiffusion theory, praseodymium ions are absorbed onto the carbon fiber surface through chemical bonding, which increases the concentration of reactive functional groups due to the chemical activity of rare earth element. These reactive functional groups can improve the compatibility and reaction between carbon fibers and epoxy matrix and form a chemical combination between carbon fiber and epoxy matrix. Therefore, the increasing of amounts of oxygen-containing functional groups on the fibers plays an important role in improving the degree of adhesion at interfaces (hereby, Keesom's attraction of van der Waals force, hydrogen bonding, and the other small polar effects) between fibers and the matrix, and the ILSS of the resulting composites [17].
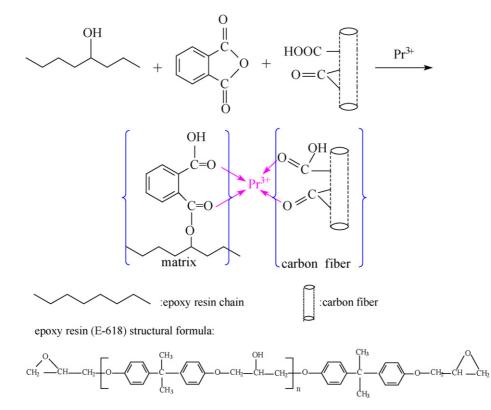

Fig. 7. Schematic diagram of coordination linkage between carbon fibers and matrix resin.

Secondly, rare earth ions adsorbed onto fiber surface form coordinate bond between fibers and matrix and act as the bridge connecting carbon fibers to matrix resin [30,31]. The schematic diagram is shown in Fig. 7.

In addition, when carbon fibers are soaked and irradiated in rare earth solution, fiber surface become rougher. Increased fiber roughness and surface striations should promote a mechanical keying or interlocking mechanism between the fibers and the matrix [5]. As a result, the interfacial adhesion of carbon fiber/epoxy composites is improved through rare earth surface treatment.

By γ-ray irradiation, the oxygen dissolved in solution is reacted with carbon fiber and the chemical bonding between rare earth element and carbon fiber surface is strengthened owing to increase of carboxyl and carbonyl. The oxygen-containing functional groups of fiber surface are changed. Therefore, the interfacial property of irradiated carbon fiber/epoxy composites is better than that of soaked carbon fiber/epoxy composites.

4. Conclusions

The treated carbon fiber surface was rougher and some granules were formed, compared to the original carbon fiber. The element of praseodymium was detected, the carbonyl carbon in ketones and quinines (C=O) and carboxyl or ester (COOH/COOR) functional groups were increased, and the graphitic carbon (C–C) and phenolic or ether oxygen (C–OH/C–O–C) functional groups were decreased after treatment. Rare earth treatments also brought about an increase in the degree of disorder on fiber surface. ILSS of carbon fiber/epoxy composites was enhanced by about 8.5% after rare earth immersion treatment. ILSS of the composites, which employed rare earth irradiation-treated carbon fibers showed about a 13.1% improvement compared with that of composites employing non-surface treated carbon fibers. This could be attributable to the increase of oxygen groups, coordination linkage between fiber and matrix and improvement of roughness. Gamma ray irradiation may be beneficial to strengthen the chemical bonding between carbon fibers and rare earth and increase the oxygen groups of fiber surface.

References

[1] M.A. Montes-Moran, A. Martinez-Alonso, J.M.D. Tascon, Carbon 39 (2001) 1057.
[2] D. Nursel, J.P. Wightman, Carbon 37 (1999) 1105.
[3] N. Dilsiz, N.K. Erinc, E. Bayramli, G. Akovali, Carbon 33 (1995) 853.
[4] A. bismarck, C. Wuertz, J. Springer, Carbon 37 (1999) 1019.
[5] Y.D. Huang, L. Liu, J.H. Qiu, Compos. Sci. Techol. 62 (2002) 2153.
[6] A. Fukunaga, S. Ueda, Compos. Sci. Techol. 60 (2000) 249.
[7] S.-J. Par, M.-K. Seo, K.-Y. Rhee, Mater. Sci. Eng. A 356 (2003) 219.
[8] A. Martinez-Villafane, J.G. Chacon-Nava, C. Gaona-Tiburcio, Mater. Sci. Eng. A 363 (2003) 15–19.
[9] Y. Xue, X. Cheng, J. Mater. Sci. Lett. 20 (2001) 1729.
[10] Y. Lin, K. Xiao, A. Zhang, J. Rare Earth 23 (2005) 720.
[11] B. He, W. Sun, M. Wang, Z. Shen, Mater. Chem. Phys. 95 (2006) 202.
[12] J. Kobelke, J. Kirchhof, K. Schuster, A. Schwuchow, J. Non-Cryst. Solids 284 (2001) 123.
[13] R.L. Satet, M.J. Hoffmann, R.M. Cannon, Mater. Sci. Eng. A 422 (2006) 66–76.
[14] X. Chen, Y. Xue, C. Xie, Mater. Lett. 57 (2003) 2553.
[15] X.H. Cheng, Y.J. Xue, C.Y. Xie, J. Rare Earth 20 (2002) 282.
[16] H. Viswanathan, Y.Q. Wang, A.A. Audi, P.J. Allen, P.M.A. Sherwood, Chem. Mater. 13 (2001) 1647.
[17] S.-K. Ryu, B.-J. Park, S.-J. Park, J. Colloid Interf. Sci. 215 (1999) 167–169.
[18] S.D. Gardner, G. He, C.U. Pittman Jr., Carbon 34 (1996) 1221.
[19] S.-J. Park, B.-J. Kim, Mater. Sci. Eng. A 408 (2005) 269.
[20] J.P. Boudou, J.I. Paredes, A. Cuesta, Carbon 41 (2003) 41.
[21] P.V. Lakshminarayanan, H. Toghiani, Carbon 42 (2004) 2433.
[22] H. Darmstadt, C. Roy, Proceedings of Carbon, vol.9, Beijing, China, 2002.
[23] J. Li, Y. Huang, Z. Wang, Z. Xu, Mater. Chem. Phys. 94 (2005) 315–320.
[24] U. Zielke, K. Huttinger, W.P. Hoffman, Carbon 34 (1996) 983–998.
[25] S.D. Gardner, G. He, C.U. Pittman Jr., Carbon 34 (1996) 1221.
[26] P.A. Lespade, A. Marchand, M. Couzi, Carbon 22 (1984) 375–385.
[27] C. Beny-Bassez, J.N. Rouzaud, Scan. Electron Microsc. 1 (1985) 119.
[28] M. Nakahara, Y. Sanada, J. Mater. Sci. 28 (1993) 1327.
[29] A. Fukunaga, T. Komami, S. Ueda, M. Nagumo, Carbon 37 (1999) 1087.
[30] W. Sun, Z. Shen, Acta Polym. Sin. 5 (2005) 641–645.
[31] L. Jin, C.-C. Wang, Acta Chim. Sin. 64 (2006) 357–362.